

MICROSTRUCTURAL ANALYSIS OF AMORPHOUS AND NANOCRYSTALLINE $Fe_{73.5-x}Cr_xNb_3Cu_1Si_{13.5}B_9$ ALLOY BY XRD ANALYSIS



M. Zashed Iqbal¹

M. A. Hossain²⁺

M. A. Gafur³

Md. Sultan Mahmud⁴

D. K. Saha⁵

S. S. Sikder⁶

¹Department of physics, Govt. Rajendra College, Faridpur, Bangladesh

²Department of physics, Khulna University of Engineering & Technology, Khulna-9203, Bangladesh

³Email: liton@phy.kuet.ac.bd

⁴(BCSIR), Dhanmondi, Dhaka-1205, Bangladesh

⁵Department of physics, The University of Asia Pacific, Dhanmondi, Dhaka-1205, Bangladesh

⁶Materials Science Division, Atomic Energy Center, Dhaka 1000, Bangladesh



(+ Corresponding author)

ABSTRACT

Article History

Received: 8 May 2018

Revised: 1 June 2018

Accepted: 5 June 2018

Published: 7 June 2018

Keywords

X ray diffractometer (XRD)

Scherrer's formula

Grain Size

Full width at half maximum

(FWHM).

This thesis is based on the experimental investigation of the effect of grain size of $Fe_{73.5-x}Cr_xNb_3Cu_1Si_{13.5}B_9$ [$x = 7, 9, 10$ & 12.5] alloys in the amorphous and annealed states. The samples are initially prepared in the amorphous state in the form of thin ribbons by rapid quenching technique at wheel speed of 25m/s in an Ar atmosphere. The alloy has been annealed in a controlled way in the temperature range of 450 - 800°C for 30 minutes. Amorphosity of the ribbon and nanocrystalline state was evaluated by XRD. In the optimized annealing condition the grain size has been obtained in the range of 11 - 30 nm. The primary crystallization phase shifts to higher annealed temperature with Cr content implying the enhancement of thermal stability of the amorphous alloys against crystallization due to increasing amount of Cr. The average grain size of the α -Fe (Si) phase, almost same under the identical annealing condition as the higher content Cr is increased. The peak shifts indicate the change of the values of Si-content of nanograins and therefore, the change of the values of lattice parameter of nanograins.

1. INTRODUCTION

Magnetism is a discipline, which stimulated by both basic and practical motivations for the study of different nanostructures. Those nanostructured materials are distinguished from conventional polycrystalline materials by the size of the crystallites that compose them. Nanomaterials are generally materials that can have one dimension, two dimension or three dimension and can be specified within a size of 100 nanometer ($1nm=10^{-9}m$). As the size reduces into the nanometer range, the materials exhibit peculiar and interesting physical, chemical, mechanical, magnetic and electrical properties compared to conventional coarse grained counterpart [1]. This new field based on nanomaterials has been named as nanotechnology and emerged as a new branch of science and technology, which is quite diverse and incorporates fields ranging from microelectronics to molecular biology [2]. But with the tremendous advancement of science and technology for the last two decades the idea that we should be able to economically arrange atoms in most of the ways permitted by physical law has gained fairly general acceptance.

In the last few decades many researchers have studied the different properties of nanomaterials [3, 4] as well as the properties of partial substitution of many elements such as Mn [5] Co [6, 7] and Cr [8] substituted ferrites. In

this study microstructural analysis of amorphous and nanocrystalline $\text{Fe}_{73.5-x}\text{Cr}_x\text{Nb}_3\text{Cu}_1\text{Si}_{13.5}\text{B}_9$ alloy has been studied by XRD Analysis.

2. MATERIALS AND METHOD

Melt spinning is a widely used production method for rapidly solidifying materials as well as preparing amorphous metallic ribbon [9, 10]. In order to prepare amorphous of $\text{Fe}_{73.5-x}\text{Cr}_x\text{Nb}_3\text{Cu}_1\text{Si}_{13.5}\text{B}_9$ [$x = 7, 9, 10$ & 12.5] alloys, the melt spinning facilities was used at the Centre for Materials Science, National University of Hanoi, Vietnam.

The Quartz crucible has in its bottom part, a rectangular nozzle tip of 8 mm length and 0.7 mm width. The position of the nozzle tip can be adjusted with respect to cooper wheel surface, so that the molten alloy was perpendicularly ejected onto the wheel surface from a distance of about 0.3 mm. The small piece of the master alloy samples were inductively remelted inside the quartz tube crucible followed by ejecting the molten metal with over pressure of 250 mbar of 99.9% pure Ar supplied from an external reservoir through a nozzle onto a rotating copper wheel with surface velocity of 30 m/sec. The temperature was monitored by an external pyrometer from the upper surface of the molten alloy through a quartz window.

The metal alloys were ejected at a temperature of about 150 to 250 K above the melting point of the alloy. The resulting ribbon samples had thickness of about 20-25 μm and width ~ 6 mm. Processing parameters such as the thermal conductivity of the rotating quench wheel, wheel speed, ejection pressure, thermal history of the melt before ejection, distance between nozzle of quartz tube and rotating wheel, as well as processing atmosphere have been influenced on the microstructure and properties of melt-spun ribbons. The lower pressure of 250 mbar as mentioned above stabilizes the turbulence between melt pull and rotating copper wheel enhancing the heat transfer resulting in a more uniform quenching. As a result, a more uniform ribbon microstructure can be obtained at relatively low wheel speed. With increasing wheel speeds for a given ejection rate, the increasing extraction rate results in thinner ribbons.

3. RESULTS AND DISCUSSION

X-ray diffraction (XRD) is generally used for the identification of various phases while the grain size is estimated by high-resolution transmission electron microscope (HRTEM) and / or by X-ray diffraction. XRD has been used to identify crystalline phase in nanocrystalline materials. Nanocrystalline alloys are above crystalline and because of their crystallinity they exhibit Bragg scattering peaks in XRD experiments. However, due to their small size, significant fine particle broadening is observed in the Bragg peaks. For 50nm particles, a broadening of 0.2° at half width the peak is expected which can easily be measured. Using Scherrer's formula of line broadening, particle size between 5 to 60nm can be measured using XRD.

In the present work, in order to study the crystallization onset temperature, XRD spectra have been recorded for the nominal composition $\text{Fe}_{73.5-x}\text{Cr}_x\text{Nb}_3\text{Cu}_1\text{Si}_{13.5}\text{B}_9$ [$x = 7, 9, 10$ & 12.5] annealed at 450° to 800° for 30 minutes. The approximately annealed samples were subjected to XRD by using a MTI Corporation built GSL-1600 x 40 tube furnace to examine the micro structural evaluation as a function of annealing temperature. From the experiment, four samples are annealed at different temperatures for 30 minute and every sample was taken under XRD analysis. From the output of XRD analysis three structural parameters such as calculated:

- (i) Lattice Parameter (a_0)
- (ii) Grain Size (D_g)
- (iii) Silicon Content (Si)
- (i) Lattice Parameter Calculation

Lattice Parameter of crystalline bcc Fe-Si nanograin was determined at different annealing temperature of the experimental alloys. Structure of the α -Fe(Si) grains depends on the annealing temperature. Normally lattice Parameter of an alloy composition is determined by the Debye-Scherrer method after extrapolation of the diffraction curve for the sample. Generally for an accurate determination of the lattice parameter a number of fundamental peaks are required but in this type of tailored materials upon crystallization only major fundamental peaks (110) is used in calculation of a_0 . We have, therefore, determined the lattice parameter using only that particular reflection using equation:

$$2d \sin \theta = n\lambda \text{ and } a_0 = d\sqrt{2} \quad (1)$$

Where $\lambda = 1.54053 \text{ \AA}$ is the wavelength of Cu- K_α radiation and a_0 is determined lattice parameter of the grain, d is the inter-planar spacing and θ is the diffraction angle.

(ii) Grain Size Determination

In 1963 Kneller and Luborsky [12] studied on nanograins. Found that the magnetic properties of isolated grains change drastically as their size is reduced to the nanometer range. When these nanometric grains are consolidated to form a nanostructured material, the magnetic properties are largely determined by the grain size and the exchange interaction between the adjacent grains. Herzer [13] successfully established the theoretical explanation on the grain size dependence of superior soft magnetic properties based on his Random Anisotropy Model (RAM) after the pioneer experimental invention of FINEMET alloy by Yoshizawa, et al. [13]. One member of series FINEMET family is the sample $\text{Fe}_{73.5-x}\text{Cr}_x\text{Nb}_3\text{Cu}_1\text{Si}_{13.5}\text{B}_9$ [$x = 7, 9, 10 \text{ \& } 12.5$], which is under the investigation of the present work.

One of the most important aims of this study was to determine crystalline grain size for all the annealing temperatures. Grain size of all annealed samples of the alloy composition was determined using Scherrer method [14]. Grain size was determined from XRD pattern of (110) reflection for different annealing temperatures at constant annealing time 30 minutes from which grain size was determined using the formula

$$D_g = \frac{0.9 \lambda}{\beta \cos \theta} \quad (2)$$

Where $\lambda = 1.54178 \text{ \AA}$ is the wavelength of Cu- K_α radiation, θ is the diffraction angle and β is the full width at half maximum (FWHM) of diffraction peak in radian for different steps of annealing temperature.

(iv) Si Content in Nanograins:

The major elements of the amorphous ribbon were Fe and Si with concentration of 61 to 66.5 at. % Fe and 13.5 at. % Si. Crystalline nanograins were formed on the ribbon in the process of annealing temperature with the alloy composition of Fe-Si. It is therefore important to determine the concentration of Fe, Cr and Si in the nanograin. As lattice parameter of the nanograins have been measured for different heat treatment conditions, it is easy to calculate the Si content in the nanograin from the quantitative relationship between lattice parameter (a) and Si-content (Si at.%) developed by Bozorth [15]. It is easy to calculate the Si content in the nanograin from the Pearson hand book relationship [16]. From this relationship we have considered a simple equation to calculate Si-content from lattice parameter. This equation is

$$b = -467a_0 + 1342.8 \quad (3)$$

where b is at. % Si in the nanograins, a_0 is the lattice parameter of nanograins.

3.1. XRD Analysis of the Nanocrystalline Ribbon with Composition

$\text{Fe}_{66.5}\text{Cr}_7\text{Nb}_3\text{Cu}_1\text{Si}_{13.5}\text{B}_9$

In the present work, structure of the $\text{Fe}_{66.5}\text{Cr}_7\text{Nb}_3\text{Cu}_1\text{Si}_{13.5}\text{B}_9$ nanocrystalline ribbon alloys annealed at temperature (T_a) from 450°C to 800°C for annealing time 30 minutes are investigated by the XRD method are presented in Fig. 5.14. It is evident from Fig. 5.14 when the sample annealed below 550°C i.e. at 550°C, it exhibit only one broad peak around $\theta = 45^\circ$ at the position of d_{110} reflection which is generally known as diffuse hallow. This diffuse hallow indicates the amorphous nature of the sample. It means at the annealing temperature below 550°C, no crystalline peak has been detected. Patterns of $T_a=550^\circ\text{C}$ indicates a clear bcc $\alpha - \text{Fe}(\text{Si})$ of said compositions after heat treatment for 30 minutes. The same pattern observed for all the samples at different annealing temperatures indicates the $\alpha - \text{Fe}(\text{Si})$ phase. The crystallization onset temperature from DTA experiments for different heating rates, were formed in the range of 400°C to 800°C, which shows a good consistency with the XRD results. The XRD pattern has taken for the samples annealed from 450°C to 800°C under the same condition. The intensity of the diffracted peak of $\alpha - \text{Fe}(\text{Si})$ phase in the alloy is increased with the increase of annealing temperature. For an annealing at higher temperature i.e. 550°C 600°C 650°C 700°C 750°C and 800°C, the $\alpha - \text{Fe}(\text{Si})$ phase were found at the lower values of 2θ at. % 45.008°, 44.942°, 44.938°, 44.918°, 44.89° and 44.95° respectively with 100% peak intensity on (110) line. The other two fundamental peaks are corresponding to $\alpha - \text{Fe}(\text{Si})$ on (200) and (211) at $2\theta = 65.81^\circ$ and 83.69° around to bcc Fe (Si) phase. But due to their low intensity; there are not clearly visible before 650°C annealing. The balance of composition is maintained by the distribution of amorphous phase in the system.

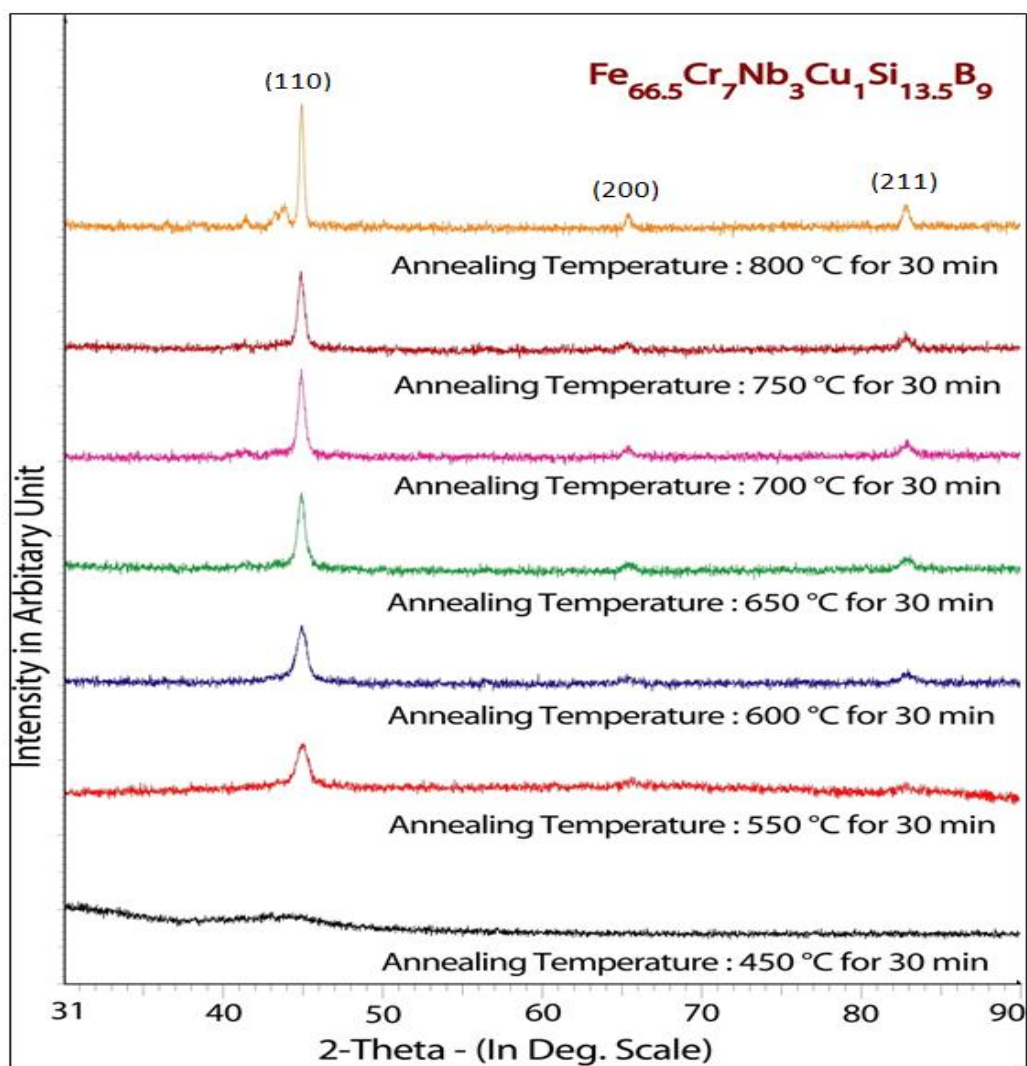


Figure-1. XRD spectra of $\text{Fe}_{66.5}\text{Cr}_7\text{Nb}_3\text{Cu}_1\text{Si}_{13.5}\text{B}_9$ alloys of annealed at different temperatures at constant annealing time 30 min
 Source: PHILIPS X' Pert PRO X-ray diffractometer, Material Science Division, Atomic Energy Center, Dhaka, Bangladesh.

From DTA result it is expected that boride phase would form beyond 580.6°C but the formation of crystalline phase other than $\text{Fe}(\text{Si})$ in the XRD pattern has not been detected for T_a up to around 550°C for the sample as expected from the DTA analysis of samples. The XRD patterns illustrated in Fig. 5.14 reveal that the difference in the Bragg's peak as well as the intensity of the fundamental reflections become gradually stronger as the temperature of the heat treatment increases. This increase in the sharpness of the intensity peaks with the annealing temperature indicates that crystalline volume fraction has been increases and also grains become coarser with increased spectra of the thermally treated samples of Cr substituted FINEMET's evidence of $\alpha - \text{Fe}(\text{Si})$ and Fe_2B crystalline phases might be found along with iron oxides ($\alpha - \text{Fe}_2\text{O}_3$ and $\lambda - \text{Fe}_2\text{O}_3$) of less than 1% of the total composition [13]. The reason of oxide formation lies in fact of performing annealing in air atmosphere. In spite of addition of refractory elements it should be suggested that the heat treatment should be done in an inert (non-reactive) atmosphere to avoid oxidation and other reactions.

The intensity of the diffracted peak of $\alpha - \text{Fe}(\text{Si})$ phase in the alloy is increased with the increase of annealing temperature. The systematic but negligible shift of the peak forwards the larger angles with increasing temperature indicates that lattice parameter of the phase gradually decreases due to the increase of Si-content of the

$\alpha - Fe(Si)$ phase. Both the decrease in lattice parameter and increase in intensity of the fundamental peak with increasing annealing temperature suggest that Si-atom diffuse most intensively into the bcc-Fe with increase of annealing temperature. The diffusion of Si in bcc $\alpha - Fe$ is finally found as the nanocrystalline bcc $\alpha - Fe(Si)$ lattice which is identified by XRD and therefore we see the increase intensity due to increase of the crystalline part in the alloy.

The lattice parameter, the Si-content in bcc nanograins and the grain size of bcc grain can easily be calculated from the fundamental peak of (110) reflection. All the results are shown in Table-1.

Table-1. Experimental XRD data of nanocrystalline $Fe_{66.5}Cr_7Nb_3Cu_1Si_{13.5}B_9$ for different annealing temperature

Annealing Temp. in °C	θ (deg.)	d (Å)	FWHM (deg.)	a_0 (Å)	D_g (nm)	Si (at%)
450	--	--	--	--	--	--
550	22.504	2.0141	0.765	2.8484	11	12.61
600	22.471	2.0169	0.660	2.8523	13	10.78
650	22.469	2.0171	0.485	2.5826	18	10.64
700	22.459	2.0179	0.466	2.8538	19	10.08
750	22.445	2.0111	0.460	2.8555	19	9.28
800	22.475	2.0166	0.311	2.8518	28	11.01

Source: PHILIPS X' Pert PRO X-ray diffractometer, Material Science Division, Atomic Energy Center, Dhaka, Bangladesh.

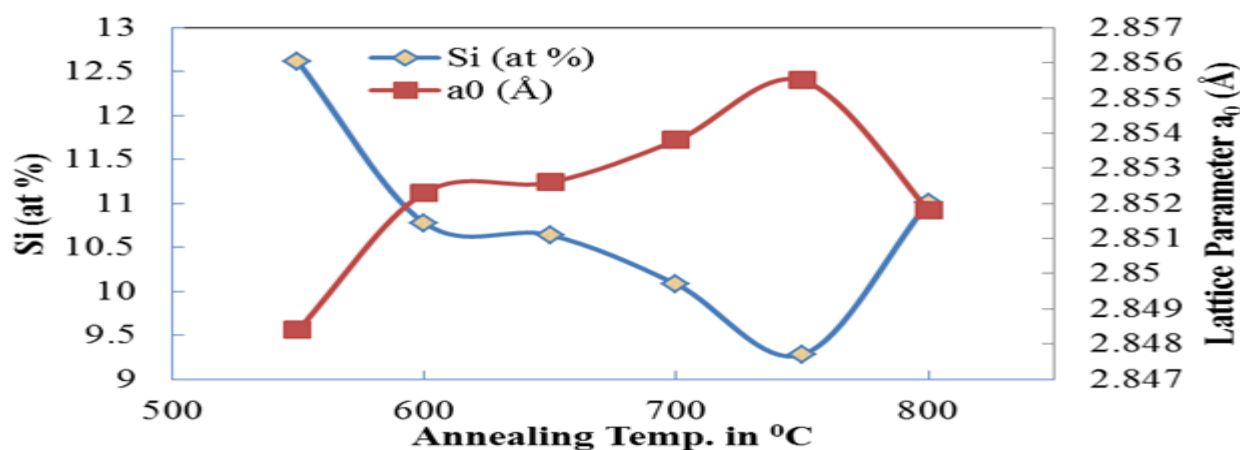


Figure-2. Change of Si (at. %) content and Lattice Parameter with different annealing temperature for the sample with composition $Fe_{66.5}Cr_7Nb_3Cu_1Si_{13.5}B_9$

Source: PHILIPS X' Pert PRO X-ray diffractometer, Material Science Division, Atomic Energy Center, Dhaka, Bangladesh.

Figure-2 shows the lattice parameter of $\alpha - Fe(Si)$ crystallites embedded in the amorphous matrix of various annealed samples in the temperature from 550°C to 800°C has been performed. With the increases of annealing temperature lattice parameter increases gradually up to 750°C above this temperature decreases. The lattice parameter of $\alpha - Fe(Si)$ phase is always smaller than that of pure Fe, the value of which is 2.8664 Å [17]. When the annealing temperature is above 750°C there is a decrease of lattice parameter due to the contraction of $\alpha - Fe$ lattice as a result of diffusion of the Si with smaller grain size from a substitution solid solution during the crystallization process of $\alpha - Fe(Si)$. The Si-contents of the alloy $Fe_{66.5}Cr_7Nb_3Cu_1Si_{13.5}B_9$ at different annealing temperature 550°C to 800°C for 30 minutes annealing time are found to be in the range of 9.28% to 12.61%. All these results are presented in Table-1 and the pattern of change in Si-content with respect to annealing temperature

is presented in Figure-2. Percentage of Si is the controlling parameter of structural change for the nanocrystalline alloy. Percentage of Si in the $Fe(Si)$ phase has a point of saturation i.e. maximum value. For this sample it is about 9.28% Si and obtained at 750°C. Above this critical temperature of Si increases i.e. lattice parameter decreases. So Si-content and lattice parameter is closely related which is expressed in Pearson Hand book relationship [16].

Instrumental broadening of the system was determined from $\theta - 2\theta$ scan of standard Si. At the position of (110) reflections, the value of instrumental broadening was found to be 0.07°. This value instrumental broadening was obtained FWHM value of each peak. Asymmetrical broadening of the peak due to stacking fault of bcc crystal was corrected negligible in the present case. All determined grain size was values for every step of heat treatment are listed in Table-1. In Figure- 2 it is clear that at low annealing temperature 550°C, the FWHM of the peak is large and with the increases of annealing temperature, the values of FWHM are getting smaller. The peaks are, therefore becoming sharper with the shifting the peak position towards higher 2θ value. The peak shifts indicate the change of the values of Si-content of nanograins and therefore, the change of the values of lattice parameter of nanograins.

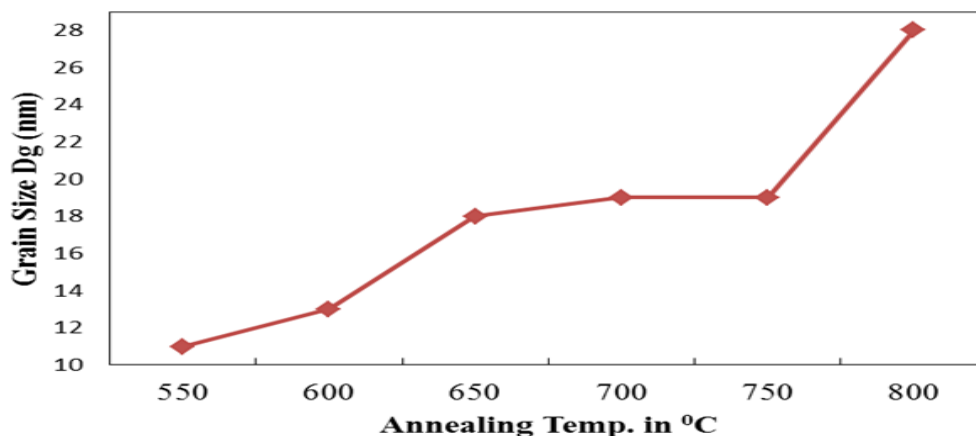


Figure-3. Change of Grain Size with different annealing temperature for the sample with composition $Fe_{66.5}Cr_7Nb_3Cu_1Si_{13.5}B_9$
Source: PHILIPS X' Pert PRO X-ray diffractometer, Material Science Division, Atomic Energy Center, Dhaka, Bangladesh.

Figure-3 and Table-1 that grain size increases with annealing temperature from a value of $D_g = 11$ nm for $T_a = 550^\circ\text{C}$ to $D_g = 28$ nm for the sampled annealed at $T_a = 800^\circ\text{C}$ while Si-content decreases with annealing temperature. The increases of annealing temperature initiates partitioning of Si in the bcc Fe phase and thus grain growth due to formation of nanocrystalline bcc Fe (Si) grains. In the range of annealing temperature 550°C to 750°C, the grain size remains in the range of 11 to 19 nm corresponding to soft magnetic bcc Fe(Si) phases. Above 750°C, grain grow rapidly at attain value of 28 nm at 800°C indicating formation of Fe_2B phase. Formation of boride phase is detrimental to soft magnetic properties. Thus fact reveals that heat treatment temperature should be limited with 650°C to 750°C to obtain soft magnetic behavior, which will be clear that constant grain size. The formation of the nanometric microstructure corresponding to the grain growth with increase of annealing temperature is ascribed to combined effects of Cu and Nb and their low solubility in Fe. Cu which is insoluble in $\alpha - Fe(Si)$, segregates prior to at the very beginning of nanocrystallization forming Cu-rich clusters and the nucleation of Fe(Si) grains is thought to be multiplied by clustering of Cu which stands as the reason for the grain growth at the initial stage of crystallization. It was observed that grain size 11nm for the sample annealed at 550°C for 30 minutes to a limiting value of 13-19 nm between annealing temperature 600°C to 750°C.

3.2. XRD Analysis of the Nanocrystalline Ribbon with Composition $Fe_{64.5}Cr_9Nb_3CuSi_{13.5}B_9$

Figure-4 shows typical XRD patterns of bcc $\alpha - Fe(Si)$ phase for the sample of composition $Fe_{64.5}Cr_9Nb_3CuSi_{13.5}B_9$ after heat treatment (30 minutes) at different temperature. From 450°C to 800°C pattern of $T_a = 450^\circ C$ & $550^\circ C$ indicates the amorphous nature. After heat treatment at $T_a = 600^\circ C$ initiation of crystallization takes place. The same patterns were observed for all samples at different annealing temperature indicating the bcc $\alpha - Fe(Si)$ phase which are developed on amorphous ribbon after heat treatment. Moreover, the bcc Fe-phase is unique crystalline of the alloys annealed at 600°C to 800°C, the variation of intensity of the diffraction lines in patterns obtained under the same condition, reveals that the peak of bcc Fe-phase in the alloys is increased with increase of the annealing temperature of crystalline nanograin of bcc Fe (Si) phase. All the results of θ , d-value, FWHM, a_0 , D_g and Si (at. %) at different annealing temperature of these composition are listed in Table-2. For a annealing at higher temperature i.e., 600°C, 650°C, 700°C, 750°C and 800°C, the $\alpha - Fe(Si)$ phase were found at the lower values of 2θ at % 45.46°, 44.92°, 44.8°, 44.989° and 44.908° respectively with 100% peak intensity on (110) line. The other two fundamental peaks corresponding to $\alpha - Fe(Si)$ on (200) and (211) diffraction line for annealing temperatures at and above 650°C is obtained in this Figure-3. But due to their low intensity, they are not clearly visible before 600°C annealing.

In the Figure-5 the lattice parameter of $\alpha - Fe(Si)$ crystallites embedded in the amorphous matrix of various annealed samples in the temperature range between 600°C to 800°C has been performed. With the increase of annealing temperature lattice parameter increases gradually up to 700°C above this temperature decreases. The lattice parameter of $\alpha - Fe(Si)$ phase is always smaller than that of pure-Fe, the value of which is 2.8664 Å. The Si-content of the alloy $Fe_{64.5}Cr_9Nb_3CuSi_{13.5}B_9$ at different annealing temperature 600°C to 800°C at constant annealing time 30 minutes are found to be in the range of 9.00% to 10.87%. All these results are presented in Table-2 and the pattern of change in Si-content with respect to annealing temperature is presented in Figure-6. It is observed that the Si-content in $\alpha - Fe(Si)$ phase decreases with increases annealing temperature up to 700°C and above then Si-content increases again. Above or below this critical annealing temperature % Si decreases as lattice parameter increases. In Table-2 it is clear that with the increase of annealing temperature the value of FWHM decreases. The peak is, therefore, getting sharper with the shifting of peak position forwards higher 2θ value.

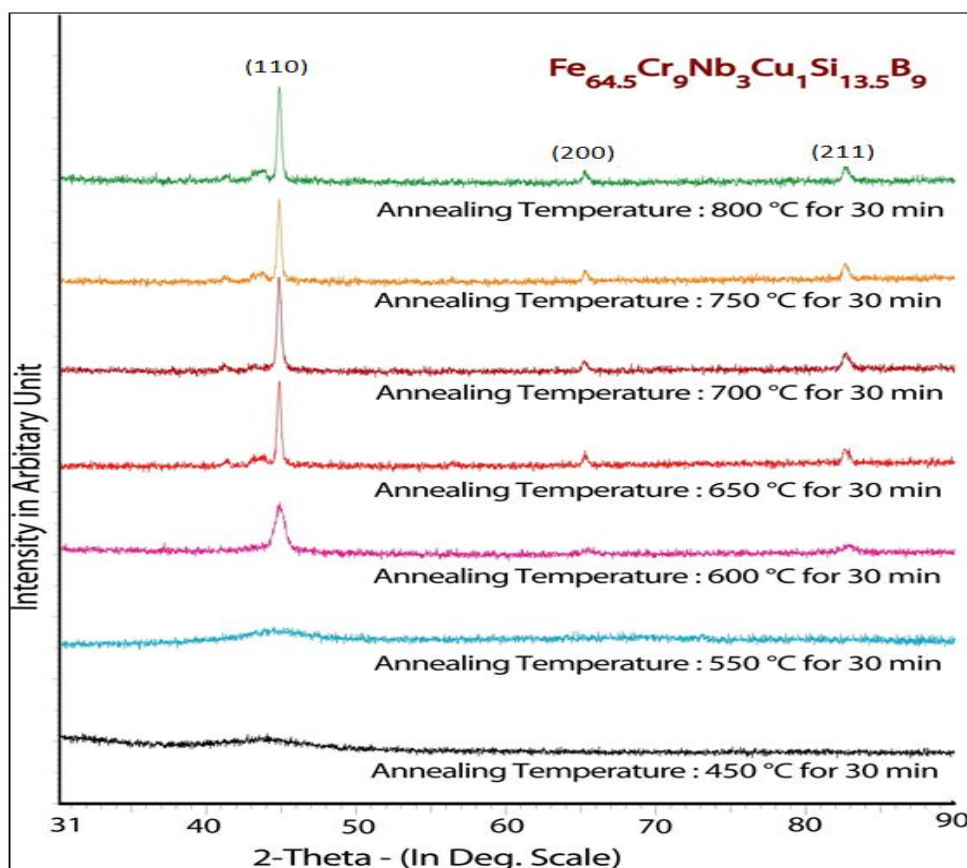


Figure-4. XRD spectra of $Fe_{64.5}Cr_9Nb_3Cu_1Si_{13.5}B_9$ alloys of annealed at different temperature at constant annealing time 30 min
 Source: PHILIPS X' Pert PRO X-ray diffractometer, Material Science Division, Atomic Energy Center, Dhaka, Bangladesh.

Table-2. Experimental XRD data of nanocrystalline $Fe_{64.5}Cr_9Nb_3Cu_1Si_{13.5}B_9$ amorphous ribbon at different annealing temperatures

Annealing Temp. in °C	θ (deg.)	d (Å)	FWHM (deg.)	a_0 (Å)	D_g (nm)	Si (at %)
450	--	--	--	--	--	--
550	--	--	--	--	--	--
600	22.473	2.0167	0.653	2.8521	13	10.87
650	22.460	2.0178	0.307	2.8536	28	10.17
700	22.440	2.0195	0.315	2.8561	27	09.00
750	22.449	2.0188	0.288	2.8550	30	09.52
800	22.454	2.0183	0.287	2.8544	30	09.81

Source: PHILIPS X' Pert PRO X-ray diffractometer, Material Science Division, Atomic Energy Center, Dhaka, Bangladesh.

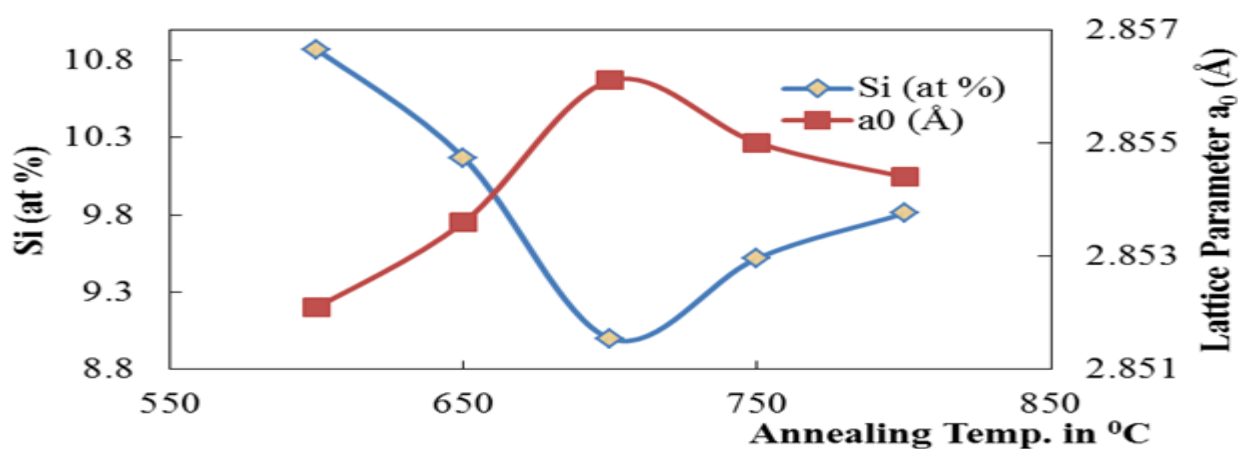


Figure-5. Change of Si (at %) content and Lattice Parameter with different annealing temperature for the sample with composition $Fe_{64.5}Cr_9Nb_3Cu_1Si_{13.5}B_9$

Source: PHILIPS X' Pert PRO X-ray diffractometer, Material Science Division, Atomic Energy Center, Dhaka, Bangladesh.

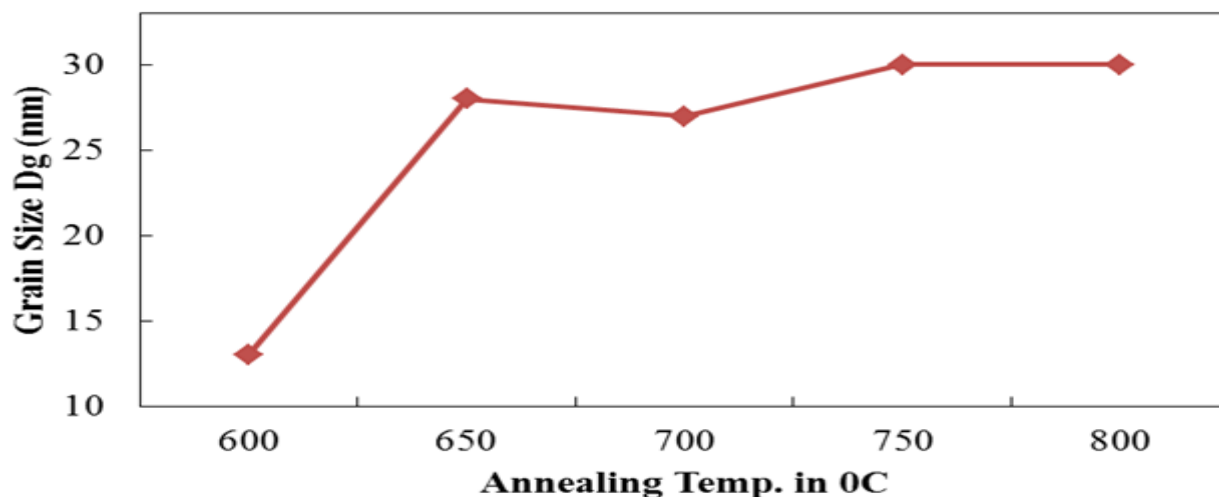


Figure-6. Change of Grain Size with different annealing temperature For the sample with composition $\text{Fe}_{64.5}\text{Cr}_9\text{Nb}_3\text{Cu}_1\text{Si}_{13.5}\text{B}_9$
 Source: PHILIPS X' Pert PRO X-ray diffractometer, Material Science Division, Atomic Energy Center, Dhaka, Bangladesh.

In Figure-6 the mean grain size of the nanograins determined from the X-ray fundamental line (110) using the Scherrers formula are presented. The increasing of annealing temperature initiates partitioning of Si in the bcc Fe phase and thus grain growth due to formation of nanocrystalline bcc Fe(Si) grains. In the range of annealing temperature 600°C to 800°C, the grain size remains in the range 13 to 30 nm. These facts reveal that heat treatment temperature should be limited with 650°C to 800°C to obtained soft magnetic behavior which will be clear that nearly constant grain size.

3.3. XRD Analysis of the Nanocrystalline Ribbon with Composition $\text{Fe}_{63.5}\text{Cr}_{10}\text{Nb}_3\text{Cu}_1\text{Si}_{13.5}\text{B}_9$

The XRD patterns for the $\text{Fe}_{63.5}\text{Cr}_{10}\text{Nb}_3\text{Cu}_1\text{Si}_{13.5}\text{B}_9$ annealed at temperature (T_a) 450°C, 550°C, 600°C, 650°C, 700°C, 750°C and 800°C each for 30 minutes are presented in Fig. 5.20. Form 450°C to 800°C pattern of $T_a = 450^\circ\text{C}$ and 550°C indicates the amorphous nature. Due to annealing at 600°C, the first crystallization peak was found at the angle 45.04°. It means at the annealing temperature below 600°C, no crystalline peak has been detected. After heat treatment at $T_a = 600^\circ\text{C}$ initiation of crystallization takes place. For annealing at higher temperature i.e., 600°C, 650°C, 700°C, 750°C and 800°C, the bcc $\alpha - \text{Fe}(\text{Si})$ phase were found at the lower values of 2θ at % 45.04°, 44.902°, 44.852°, 44.864° and 44.896° respectively with 100% peak intensity on (110) line. The other two fundamental peaks corresponding to $\alpha - \text{Fe}(\text{Si})$ on (200) and (211) diffraction line for annealing temperatures at and above 650°C is obtained in this Figure. But due to their low intensity, they are not clearly visible before 600°C annealing. The balance of composition is obtained by distribution of amorphous phase in the system.

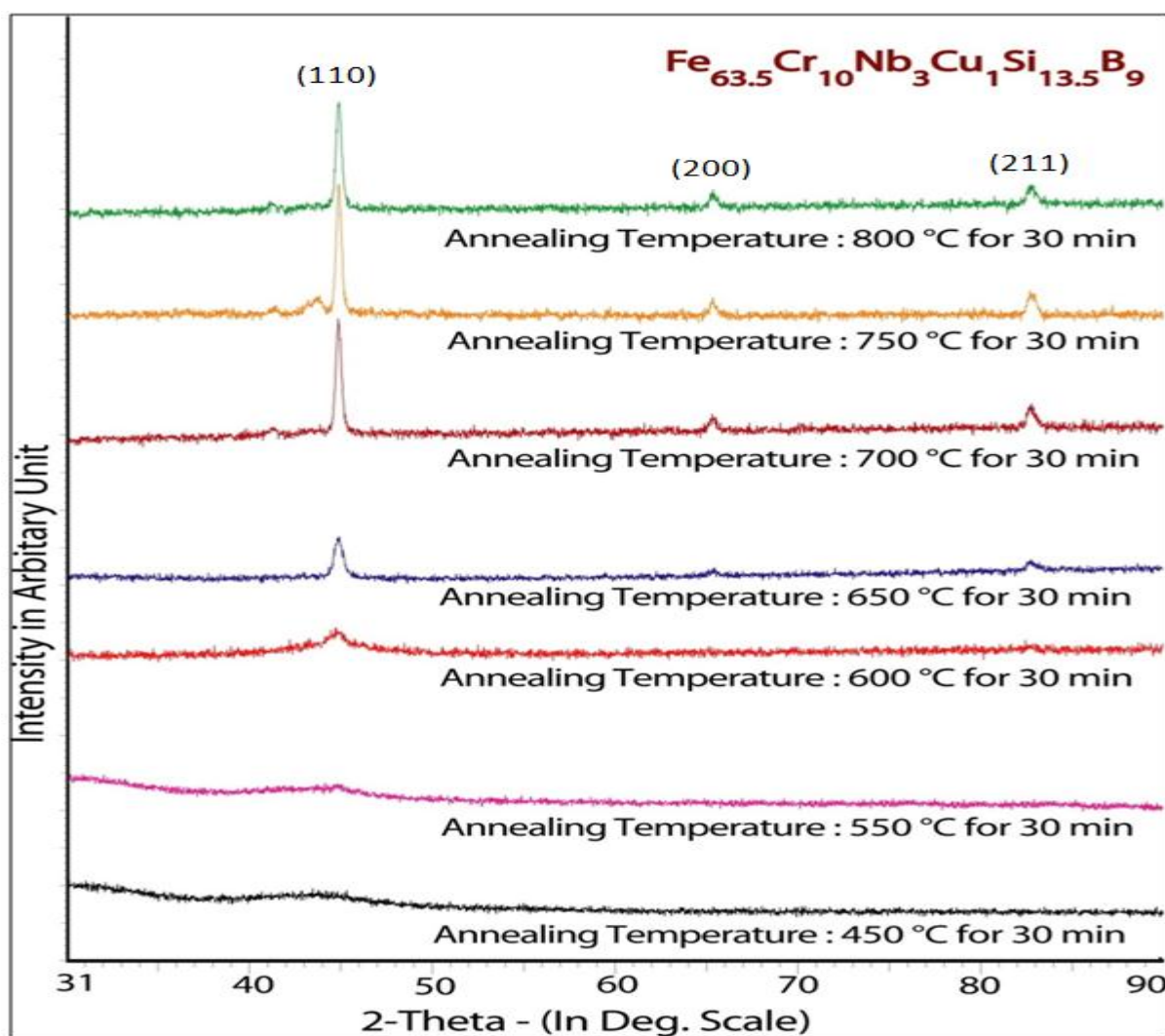


Figure-7. XRD spectra of $\text{Fe}_{63.5}\text{Cr}_{10}\text{Nb}_3\text{Cu}_1\text{Si}_{13.5}\text{B}_9$ alloys of annealed at different temperatures at constant annealing time 30 min
 Source: PHILIPS X' Pert PRO X-ray diffractometer, Material Science Division, Atomic Energy Center, Dhaka, Bangladesh.

The XRD patterns illustrated in Figure-7 reveals that the difference in the Bragg's peak as well as the intensity of the fundamental reflections becomes gradually stronger as the temperature of the heat treatment increases. This increase in the sharpness of the intensity peaks with the annealing temperature indicates that crystalline volume fraction has been increased and also grains become coarser with increased crystallinity. The systematic but negligible shift of peak forwards the larger angles with decreasing temperature indicates that lattice parameter of the phase gradually increases due to the decreasing of Si-content of the $\alpha - \text{Fe}(\text{Si})$ phase. The lattice parameter, the Si-contents in bcc nanograins and the grain size of bcc grain can easily be calculated from the fundamental peak of (110) reflection. All the results are shown in Table -3.

Table-3. Experimental XRD data of nanocrystalline $\text{Fe}_{63.5}\text{Cr}_{10}\text{Nb}_3\text{Cu}_1\text{Si}_{13.5}\text{B}_9$ amorphous ribbon at different annealing temperatures

Annealing Temp. in °C	θ (deg.)	d (Å)	FWHM (deg.)	a_0 (Å)	D_g (nm)	Si (at. %)
450	--	--	--	--	--	--
550	--	--	--	--	--	--
600	22.520	2.0127	0.737	2.8464	12	13.53
650	22.451	2.0186	0.525	2.8547	16	09.66
700	22.426	2.0207	0.344	2.8578	25	08.21
750	22.432	2.0202	0.340	2.8570	29	08.58
800	22.448	2.0189	0.332	2.8551	26	09.47

Source: PHILIPS X' Pert PRO X-ray diffractometer, Material Science Division, Atomic Energy Center, Dhaka, Bangladesh.

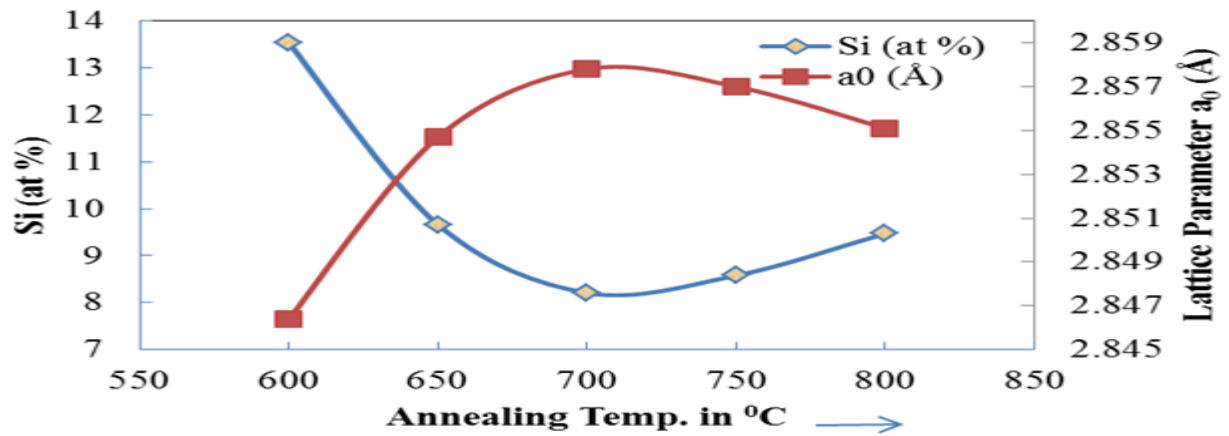


Figure-8. Change of Si (at. %) content and Lattice Parameter with different annealing temperature for the sample with composition $Fe_{63.5}Cr_{10}Nb_3Cu_1Si_{13.5}B_9$

Source: PHILIPS X' Pert PRO X-ray diffractometer, Material Science Division, Atomic Energy Center, Dhaka, Bangladesh.

Figure- 8 shows that, with the increase in annealing temperature lattice parameter increasing up to 700°C, above the annealing temperature decreases. The lattice parameter of pure Fe is 2.8664Å. But the lattice parameter at various annealing temperature for the present alloy are significantly less than that of pure Fe. It is notable that Si-contents in the nanocrystallites at different annealing temperatures are higher than Si-content of the amorphous precursor which 13.53 at %. The percentage of partitioned Si in the nanocrystalline $\alpha - Fe(Si)$ phase is maximum at 600°C. After 600°C, decrease in Si-content is observed up to 700°C, explained by the fact that at higher temperatures silicon diffuses out of nanograins due to crystallization corresponding to formation of boride phase which is consistent with the result of other FINEMET's. Figure-8 presents the inverse relationship between lattice parameter and Silicon content. When the sample up to 700°C, the increase of lattice parameter with subsequent decrease of Si-content, as showed in Figure-8 indicates that silicon diffuse out of $\alpha - Fe(Si)$ grains for which the size of $\alpha - Fe$ lattice is regained.

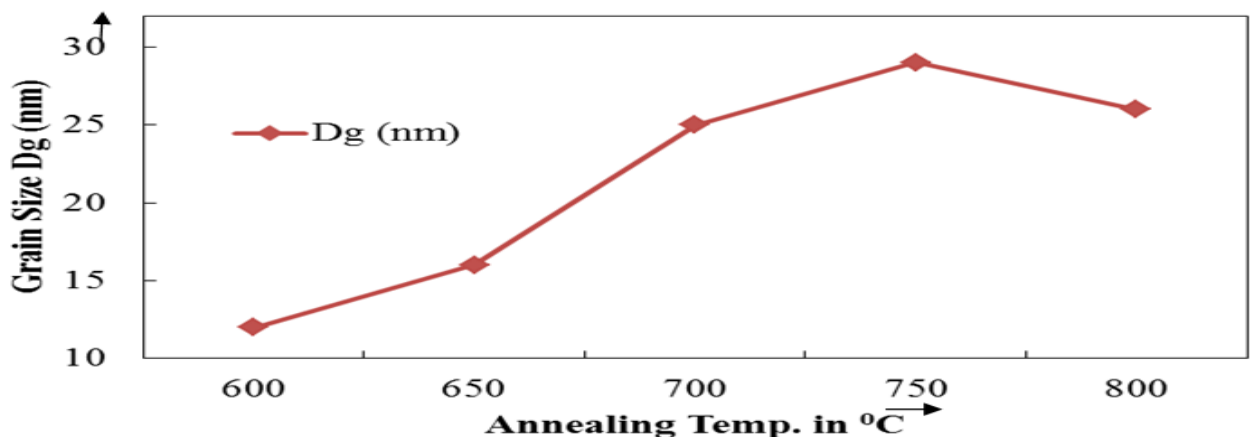


Figure-9. Change of Grain Size with different annealing temperature for the sample with composition $Fe_{63.5}Cr_{10}Nb_3Cu_1Si_{13.5}B_9$

Source: PHILIPS X' Pert PRO X-ray diffractometer, Material Science Division, Atomic Energy Center, Dhaka, Bangladesh.

From Figure-9 and Table-3 that grain size decreases with annealing temperature up to 750°C and above this annealed temperature grain size increase. In the range of annealing temperature 600°C to 800°C, the grain size remains in the range of 12 to 29 nm. Grain growth rapidly and attain value of 25 nm at 700°C indicating formation of boride phase. Formation of boride phase is detrimental to soft magnetic properties. These facts reveal that heat

treatment temperature should be limited within 600°C to 650°C to obtain optimum soft magnetic behavior, which will be clear that nearly same grain size.

3.4. XRD Analysis of the Nanocrystalline Ribbon with composition $\text{Fe}_{61}\text{Cr}_{12.5}\text{Nb}_3\text{Cu}_1\text{Si}_{13.5}\text{B}_9$

Figure-10 shows typical XRD patterns of bcc $\alpha - \text{Fe}(\text{Si})$ phase for the sample of composition $\text{Fe}_{61}\text{Cr}_{12.5}\text{Nb}_3\text{Cu}_1\text{Si}_{13.5}\text{B}_9$ after heat treatment (30 minutes) at different annealing temperature (T_a). From 450°C to 800°C pattern of $T_a = 450^\circ\text{C}$ to 600°C indicates are the amorphous nature. After heat treatment at $T_a = 650^\circ\text{C}$ initiation of crystallization takes place. The same patterns were observed for all samples at different annealing temperature indicating the bcc $\alpha - \text{Fe}(\text{Si})$ phase which are developed on amorphous ribbon after heat treatment.

For a annealing at higher temperature i.e., 650°C, 700°C, 750°C and 800°C, the bcc $\alpha - \text{Fe}(\text{Si})$ phase were found

at the lower values of 2θ at % 44.82°, 44.788°, 44.82° and 44.864° respectively with 100% peak intensity on (110)

line. The other two fundamental peaks corresponding to $\alpha - \text{Fe}(\text{Si})$ on (200) and (211) diffraction line for

annealing temperatures at and above 700°C is obtained in this figure. But due to their low intensity, they are not

clearly visible before 700°C annealing. The balance of composition is obtained by distribution of amorphous phase

in the system. The XRD patterns illustrated in Figure-10 reveals that the difference in the Bragg's peak as well as

the intensity of the fundamental reflections becomes gradually stronger as the temperature of the heat treatment

increases. All the results of θ , d-value, FWHM, lattice parameter a_0 , the grain size (D_g) and the Si-content in bcc

nanograins (at. %) can easily calculated from the fundamental peak of (110) reflection. All the results are shown in

Table- 4.

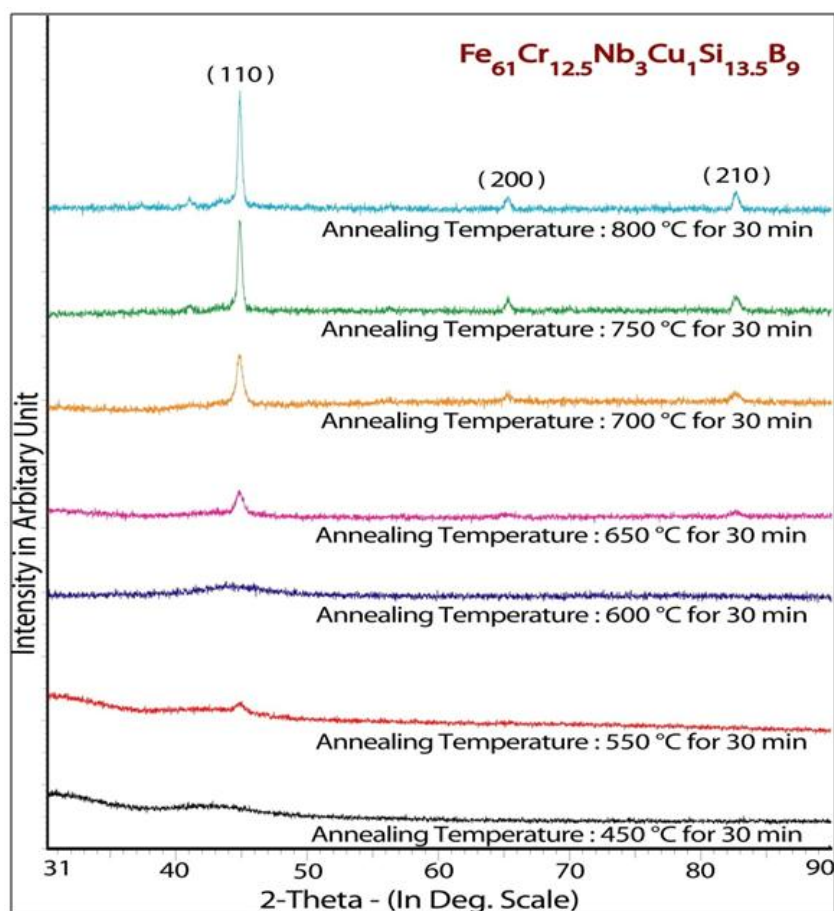


Figure-10. XRD spectra of $Fe_{61}Cr_{12.5}Nb_3Cu_1Si_{13.5}B_9$ alloys of annealed at different temperature at constant annealing time 30 min
 Source: PHILIPS X' Pert PRO X-ray diffractometer, Material Science Division, Atomic Energy Center, Dhaka, Bangladesh.

Table-4. Experimental XRD data of nanocrystalline $Fe_{61}Cr_{12.5}Nb_3Cu_1Si_{13.5}B_9$ amorphous ribbon at different annealing temperatures

Annealing Temp. in °C	θ (deg.)	d (Å)	FWHM (deg.)	a_0 (Å)	D_g (nm)	Si (at. %)
550	--	--	--	--	--	--
600	--	--	--	--	--	--
650	22.410	2.0201	0.556	2.8597	16	07.32
700	22.394	2.0235	0.524	2.8616	16	06.43
750	22.410	2.0221	0.349	2.8597	25	07.32
800	22.432	2.0202	0.296	2.8570	29	08.28

Source: PHILIPS X' Pert PRO X-ray diffractometer, Material Science Division, Atomic Energy Center, Dhaka, Bangladesh.

Figure-11 shows that, with the increase in annealing temperature lattice parameter increasing up to 700°C, above this T_a lattice parameter drops rapidly. But a_0 at various annealing temperature for the present alloy are significantly less than that of pure Fe. The value of which is 2.8664Å. Above 700°C there is a decrease of lattice parameter due to the contraction of $\alpha - Fe$ lattice as a result of diffusion of the Si. From Figure-11 it is observed that the Si-content in $\alpha - Fe(Si)$ phase decrease with annealing temperature up to 700°C. After 700°C increase in Si-content is observed. So Si-content and lattice parameter are closely related that is expressed in Pearson Hand book. Percentage of Si-content is the controlling parameter of structural change for the nanocrystalline alloy. Figure-11 presents the inverse relationship between lattice parameter and Silicon content.

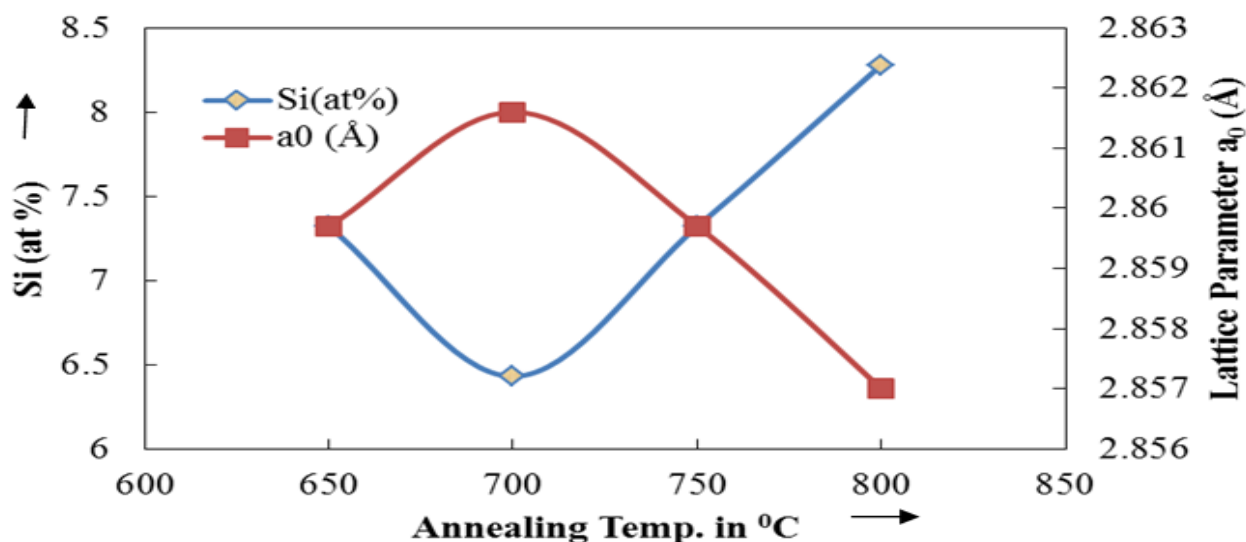


Figure-12. Change of Si (at. %) content and Lattice Parameter with different annealing temperature for the sample with composition $Fe_{61}Cr_{12.5}Nb_3Cu_1Si_{13.5}B_9$

Source: PHILIPS X' Pert PRO X-ray diffractometer, Material Science Division, Atomic Energy Center, Dhaka, Bangladesh.

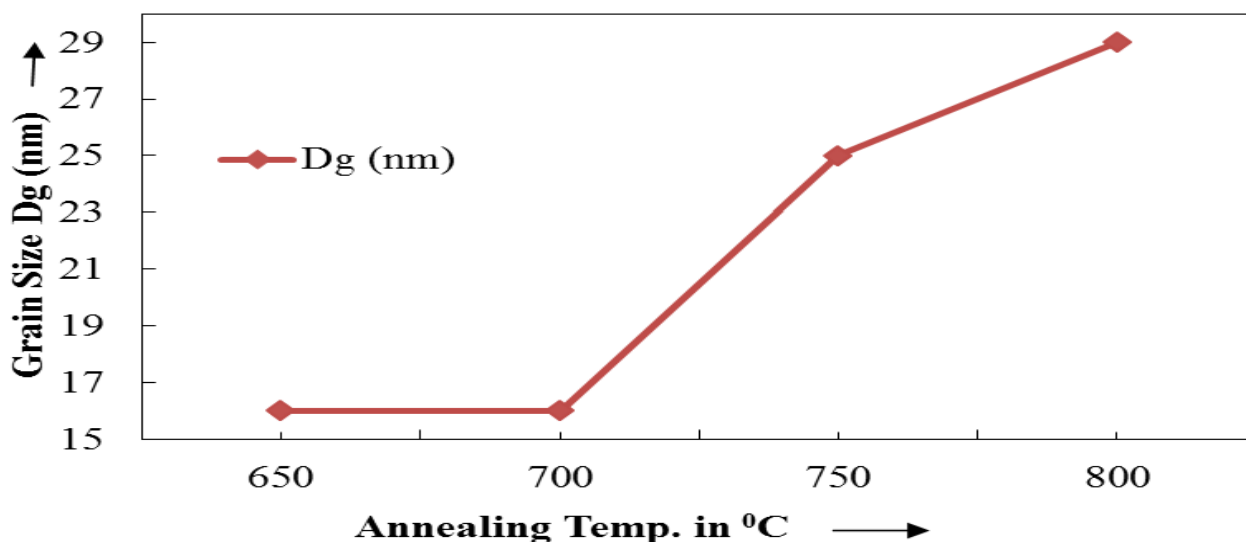


Figure-13. Change of Grain Size with different annealing temperature for the sample with composition $Fe_{61}Cr_{12.5}Nb_3Cu_1Si_{13.5}B_9$

Source: PHILIPS X' Pert PRO X-ray diffractometer, Material Science Division, Atomic Energy Center, Dhaka, Bangladesh.

From Figure-13 and Table-4 that grain size (d_g) constant up to 700°C and above this annealed temperature grain size increases. In the range of annealing temperature 650°C to 800°C, the grain size remains in the range of 16 to 29 nm. Grain growth rapidly and attain value of 25 nm at 750°C indicating formation of Boride phase. These facts reveal that heat treatment temperature should be limited within 650°C to 700°C to obtain optimum soft magnetic behavior, which will be clear that constant grain size.

4. CONCLUSION

Nanocrystalline amorphous ribbon of FINEMET family with a nominal composition $Fe_{73.5-x}Cr_xNb_3Cu_1Si_{13.5}B_9$ [$x = 7, 9, 10 \text{ \& } 12.5$] has been studied to find out the correlation between microstructural features and magnetic properties dependent on various stages of nanocrystalline during the isothermal annealing around the crystallization temperature of the amorphous stage of the as-cast ribbons has been confirmed by XRD. The evaluation of primary phase on annealed samples has been confirmed as bcc-Fe (Si) and their sizes have been determined from the line broadening of fundamental peaks (110) from XRD pattern as affected by annealing around the crystallization temperature. The temperature corresponding to the onset of crystallization obtained from the

XRD pattern is slightly lower than that of DTA data. The reason might be the two different methods of measurements. XRD measurement has been carried out on isothermal annealed samples while that of DTA on an isothermal. The grain size determined for the sample $x = 7$ from 11 to 28nm for the annealing temperature from 550°C to 800°C, $x = 9$ from 13 to 30nm for the annealing temperature from 600°C to 800°C, $x = 10$ from 12 to 29nm for the annealing temperature from 600°C to 800°C and $x = 12.5$ from 16 to 29nm for the annealing temperature from 650°C to 800°C. The higher Cr-content alloys ($x = 12.5$) do not show any sign of crystallization in their XRD pattern even at an annealing temperature of 600°C for 30 min. This is quite reasonable since their crystallization onset temperature is 650°C and higher. The lattice parameter and Si at. % shows an inverse relationship indicating that Si diffuses out of $\alpha - Fe(Si)$ grains for which the size of $\alpha - Fe$ lattice is regained.

Grain growth rapidly and attain values 19nm at 750°C for $x = 7$, 27nm at 700°C for $x = 9$, 25nm for $x = 10$ and 25nm for $x = 12.5$. For $x = 12.5$ indicating formation of boride phase (Fe_2B). The formation of boride phase is detrimental to soft magnetic properties.

Funding: The author (M. A. Hossain) is thankful to Khulna University of Engineering & Technology (KUET), Khulna, Bangladesh for the financial support.

Competing Interests: The authors declare that they have no competing interests.

Contributors/Acknowledgement: The authors are also grateful to the Materials Science Division of Atomic Energy Centre, Dhaka (AECD), Bangladesh for allowing their facilities to prepare the samples and to utilize the laboratory facilities for various measurements. Financial support from International Program in Physical Science (IPPS), Uppsala University, Sweden for this work is highly acknowledged.

REFERENCES

- [1] H. Gleiter, "Nanocrystalline materials," *Progress in Materials Science*, vol. 33, pp. 223-315, 1989.
- [2] K. Judit, "Nanostructures studied by atomic force microscopy," Ph.D. Thesis, Uppsala University, Sweden, 2003.
- [3] F. Wana, T. Liua, F. Kong, A. Wang, M. Tianc, J. Song, J. Zhang, C. Chang, and X. Wang, "Surface crystallization and magnetic properties of FeCuSiBNbMo melt-spun nanocrystalline alloys," *Materials Research Bulletin*, vol. 96, p. 275-280, 2017. [View at Google Scholar](#) | [View at Publisher](#)
- [4] V. V. Tkachev, A. K. Tsesarskaya, N. V. Ilin, G. S. Kraynova, A. N. Fedorets, V. S. Plotnikov, and D. A. Polyanski, "The microstructure and magnetic properties of the Fe-Cu-Nb-Si-B finemets with different copper content," in *AIP Conference Proceedings* 2017, p. 040051.
- [5] X. Jia, Y. Li, L. Wu, and Z. Wei, "Structure and soft magnetic properties of Fe-Si-B-P-Cu nanocrystalline alloys with minor Mn addition," *AIP Advances*, vol. 8, p. 056110, 2018. [View at Google Scholar](#) | [View at Publisher](#)
- [6] O. Ohnuma, D. H. Pins, T. Abe, H. Onodera, K. Hono, and Y. Yoshizawa, "Optimization of the microstructure and properties of Co-substituted Fe-Si-B-Nb-Cu nanocrystalline soft magnetic alloys," *Journal of Applied Physics*, vol. 93, pp. 1986 – 9194, 2003. [View at Google Scholar](#) | [View at Publisher](#)
- [7] A. Fernandez, M. J. Perez, M. Tejedor, and V. Madurga, "Thermo magnetic analysis of amorphous $(Co_xFe_{1-x})_{73.5}Nb_3Cu_1Si_{13.5}B_9$ metallic glasses," *Journal of Magnetism and Magnetic Materials*, vol. 221, pp. 338-344, 2000. [View at Google Scholar](#) | [View at Publisher](#)
- [8] V. Franco, C. F. Conde, and A. Conde, "Magnetic properties and crystallization of a $Fe_{63.5}Cr_{10}Nb_3Cu_1Si_{13.5}B_9$ alloy," *Journal of Magnetism and Magnetic Materials*, vol. 203, pp. 60-62, 1999. [View at Google Scholar](#)
- [9] P. Duwez, "Trans Tech," *American Meteorological Society*, vol. 60, pp. 844-853, 1967.
- [10] P. Duwez, "Structure and properties of glassy metals," *Annual Review of Materials Research*, vol. 6, pp. 83-117, 1976. [View at Google Scholar](#) | [View at Publisher](#)
- [11] P. Duwez, "Structure and properties of glassy metals," *Annual Review of Materials Research*, vol. 6, p. 83-117, 1976. [View at Google Scholar](#) | [View at Publisher](#)

- [12] E. F. Kneller and F. E. Luborsky, "Particle size dependence of coercivity and remanence of single-domain particles," *Journal of Applied Physics*, vol. 34, pp. 656-658, 1963. [View at Google Scholar](#) | [View at Publisher](#)
- [13] Y. Yoshizawa, S. Oguma, and K. Yamachi, "New Fe-based soft magnetic amorphous alloys composed of ultrafine grain structure," *Journal of Applied Physics*, vol. 64, pp. 6044-6046, 1988. [View at Google Scholar](#) | [View at Publisher](#)
- [14] B. D. Cullity, *Elements of X-ray diffraction*. London, England: Adison-Wisley Publishing Company Inc, 1959.
- [15] Bozorth, *Ferromagnetism*. Princeton, NJ: D. Van Norstrand Company, Inc, 1964.
- [16] W. B. Pearson, *A Hand book of Lattice spacing and Structures of metals and alloys*. London, UK: Oxford Pergamon, 1958.
- [17] M. A. Hakim and H. S. Manjura, "Effect of structural parameters on Soft Magnetic properties of two phase nanocrystalline alloy of Fe_{73.5}Cu₁Ta₃Si_{13.5}B₉," *Journal of Magnetism and Magnetic Materials*, vol. 284, pp. 395-402, 2004. [View at Google Scholar](#) | [View at Publisher](#)

Views and opinions expressed in this article are the views and opinions of the author(s), Journal of Asian Scientific Research shall not be responsible or answerable for any loss, damage or liability etc. caused in relation to/arising out of the use of the content.